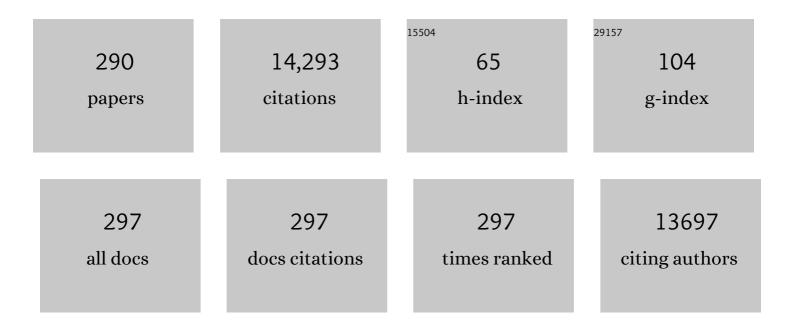
List of Publications by Year in descending order

Source: https://exaly.com/author-pdf/6926482/publications.pdf Version: 2024-02-01



#	Article	IF	CITATIONS
1	The acid dissolution characteristics of cadmium fixed by a novel Ca-Fe-Si composite material. Journal of Environmental Sciences, 2023, 127, 328-335.	6.1	0
2	Responses of ramie (Boehmeria nivea L.) to increasing rare earth element (REE) concentrations in a hydroponic system. Journal of Rare Earths, 2022, 40, 840-846.	4.8	9
3	Indicator species drive the key ecological functions of microbiota in a river impacted by acid mine drainage generated by rare earth elements mining in South China. Environmental Microbiology, 2022, 24, 919-937.	3.8	18
4	Removal pathway quantification and co-metabolic mechanism evaluation of alkylphenols from synthetic wastewater by phenolic root exudates in the rhizosphere of Phragmites australis. Journal of Hazardous Materials, 2022, 424, 127269.	12.4	1
5	Novel phytase PvPHY1 from the As-hyperaccumulator Pteris vittata enhances P uptake and phytate hydrolysis, and inhibits As translocation in Plant. Journal of Hazardous Materials, 2022, 423, 127106.	12.4	8
6	Chromium biogeochemical behaviour in soil-plant systems and remediation strategies: A critical review. Journal of Hazardous Materials, 2022, 424, 127233.	12.4	95
7	The limited exclusion and efficient translocation mediated by organic acids contribute to rare earth element hyperaccumulation in Phytolacca americana. Science of the Total Environment, 2022, 805, 150335.	8.0	17
8	Green synthesis of manganese–cobalt–tungsten composite oxides for degradation of doxycycline via efficient activation of peroxymonosulfate. Journal of Hazardous Materials, 2022, 426, 127803.	12.4	28
9	Biogeochemical cycles of nutrients, rare earth elements (REEs) and Al in soil-plant system in ion-adsorption REE mine tailings remediated with amendment and ramie (Boehmeria nivea L.). Science of the Total Environment, 2022, 809, 152075.	8.0	12
10	Enrichment and speciation of chromium during basalt weathering: Insights from variably weathered profiles in the Leizhou Peninsula, South China. Science of the Total Environment, 2022, 822, 153304.	8.0	20
11	The impact of termites on soil sheeting properties is better explained by environmental factors than by their feeding and building strategies. Geoderma, 2022, 412, 115706.	5.1	7
12	Interactions between soil protists and pollutants: An unsolved puzzle. Journal of Hazardous Materials, 2022, 429, 128297.	12.4	21
13	H3PO4 activation mediated the iron phase transformation and enhanced the removal of bisphenol A on iron carbide-loaded activated biochar. Environmental Pollution, 2022, 300, 118965.	7.5	12
14	High Fe utilization efficiency and low toxicity of Fe3C@Fe0 loaded biochar for removing of tetracycline hydrochloride in wastewater. Journal of Cleaner Production, 2022, 353, 131630.	9.3	18
15	Organic carbon and eukaryotic predation synergistically change resistance and resilience of aquatic microbial communities. Science of the Total Environment, 2022, 830, 154386.	8.0	7
16	Biogeochemical dynamics of nutrients and rare earth elements (REEs) during natural succession from biocrusts to pioneer plants in REE mine tailings in southern China. Science of the Total Environment, 2022, 828, 154361.	8.0	17
17	Natural source of Cr(VI) in soil: The anoxic oxidation of Cr(III) by Mn oxides. Journal of Hazardous Materials, 2022, 433, 128805.	12.4	33
18	Efficient purification of tetracycline wastewater by activated persulfate with heterogeneous Co-V bimetallic oxides. Journal of Colloid and Interface Science, 2022, 619, 188-197.	9.4	18

#	Article	IF	CITATIONS
19	Adsorption of Cadmium by Brassica juncea (L.) Czern. and Brassica pekinensis (Lour.) Rupr in Pot Experiment. Sustainability, 2022, 14, 429.	3.2	7
20	Effects of in situ leaching on the origin and migration of rare earth elements in aqueous systems of South China: Insights based on REE patterns, and Ce and Eu anomalies. Journal of Hazardous Materials, 2022, 435, 128959.	12.4	12
21	Inoculation of Prickly Pear Litter with Microbial Agents Promotes the Efficiency in Aerobic Composting. Sustainability, 2022, 14, 4824.	3.2	4
22	Highly dispersed Ag and g-C3N4 quantum dots co-decorated 3D hierarchical Fe3O4 hollow microspheres for solar-light-driven pharmaceutical pollutants degradation in natural water matrix. Journal of Hazardous Materials, 2022, 434, 128905.	12.4	19
23	Visualizing and assessing the size-dependent oral uptake, tissue distribution, and detrimental effect of polystyrene microplastics in Eisenia fetida. Environmental Pollution, 2022, 306, 119436.	7.5	11
24	Significance of Non-DLVO Interactions on the Co-Transport of Functionalized Multiwalled Carbon Nanotubes and Soil Nanoparticles in Porous Media. Environmental Science & Technology, 2022, 56, 10668-10680.	10.0	10
25	Aqueous aggregation and deposition kinetics of fresh and carboxyl-modified nanoplastics in the presence of divalent heavy metals. Water Research, 2022, 222, 118877.	11.3	15
26	Quantitative analysis on the redox conversion mechanism of Cr(VI) and As(III) by iron carbide based biochar composites. Chemical Engineering Journal, 2022, 446, 137417.	12.7	16
27	Chlortetracycline hydrochloride removal by different biochar/Fe composites: A comparative study. Journal of Hazardous Materials, 2021, 403, 123889.	12.4	28
28	Energy models and the process of fluid-magnetic separation for recovering cobalt micro-particles from vacuum reduction products of spent lithium ion batteries. Journal of Cleaner Production, 2021, 279, 123230.	9.3	16
29	Dynamic release and transformation of metallic copper colloids in flooded paddy soil: Role of soil reducible sulfate and temperature. Journal of Hazardous Materials, 2021, 402, 123462.	12.4	8
30	Microscopic mechanism about the selective adsorption of Cr(VI) from salt solution on O-rich and N-rich biochars. Journal of Hazardous Materials, 2021, 404, 124162.	12.4	63
31	Recovery nano-flake (100Ânm thickness) of zero-valent manganese from spent lithium-ion batteries. Journal of Cleaner Production, 2021, 278, 123867.	9.3	11
32	Biological aqua crust mitigates metal(loid) pollution and the underlying immobilization mechanisms. Water Research, 2021, 190, 116736.	11.3	17
33	Transformation behaviors and environmental risk assessment of heavy metals during resource recovery from Sedum plumbizincicola via hydrothermal liquefaction. Journal of Hazardous Materials, 2021, 410, 124588.	12.4	26
34	Enhanced adsorption of tetracycline by an iron and manganese oxides loaded biochar: Kinetics, mechanism and column adsorption. Bioresource Technology, 2021, 320, 124264.	9.6	147
35	A novel technology of recovering magnetic micro particles from spent lithium-ion batteries by ultrasonic dispersion and waterflow-magnetic separation. Resources, Conservation and Recycling, 2021, 164, 105172.	10.8	22
36	Variation in rare earth element (REE), aluminium (Al) and silicon (Si) accumulation among populations of the hyperaccumulator Dicranopteris linearis in southern China. Plant and Soil, 2021, 461, 565-578.	3.7	18

#	Article	IF	CITATIONS
37	Rare earth elements, aluminium and silicon distribution in the fern <i>Dicranopteris linearis</i> revealed by μPIXE Maia analysis. Annals of Botany, 2021, 128, 17-30.	2.9	12
38	Quantification of nickel and cobalt mobility and accumulation via the phloem in the hyperaccumulator <i>Noccaea caerulescens</i> (Brassicaceae). Metallomics, 2021, 13, .	2.4	3
39	Effects of zinc oxide nanoparticles on antioxidants, chlorophyll contents, and proline in Persicaria hydropiper L. and its potential for Pb phytoremediation. Environmental Science and Pollution Research, 2021, 28, 34697-34713.	5.3	31
40	Industrial Ramie Growing on Reclaimed Ion-Adsorption Rare Earth Elements Mine Tailings in Southern China: Defibration and Fibers Quality. Waste and Biomass Valorization, 2021, 12, 6255-6260.	3.4	5
41	Non-monotonic contribution of nonionic surfactant on the retention of functionalized multi-walled carbon nanotubes in porous media. Journal of Hazardous Materials, 2021, 407, 124874.	12.4	6
42	In situ N-doped carbon-coated mulberry-like cobalt manganese oxide boosting for visible light driving photocatalytic degradation of pharmaceutical pollutants. Chemical Engineering Journal, 2021, 411, 128497.	12.7	50
43	Phenomic and metabolomic responses of roots to cadmium reveal contrasting resistance strategies in two rice cultivars (Oryza sativa L.). Soil Ecology Letters, 2021, 3, 220-229.	4.5	16
44	Coupling experiments with calculations to understand the thermodynamics evolution for the sorption of zwitterionic ciprofloxacin on oxidizing-aged pyrogenic chars in the aquatic system. Journal of Hazardous Materials, 2021, 411, 125101.	12.4	4
45	Comparative analysis of sRNAs, degradome and transcriptomics in sweet sorghum reveals the regulatory roles of miRNAs in Cd accumulation and tolerance. Planta, 2021, 254, 16.	3.2	6
46	Transport and Retention of Free-Living Amoeba Spores in Porous Media: Effects of Operational Parameters and Extracellular Polymeric Substances. Environmental Science & Technology, 2021, 55, 8709-8720.	10.0	14
47	Mediation effects of different sulfur forms on solubility, uptake and accumulation of Cd in soil-paddy rice system induced by organic carbon and liming. Environmental Pollution, 2021, 279, 116862.	7.5	16
48	Substrate-dependent competition and cooperation relationships between <i>Geobacter</i> and <i>Dehalococcoides</i> for their organohalide respiration. ISME Communications, 2021, 1, .	4.2	27
49	Waste activated sludge stimulates in situ microbial reductive dehalogenation of organohalide-contaminated soil. Journal of Hazardous Materials, 2021, 411, 125189.	12.4	27
50	A new method for recovering rare earth elements from the hyperaccumulating fern Dicranopteris linearis from China. Minerals Engineering, 2021, 166, 106879.	4.3	14
51	Co-transport and retention of zwitterionic ciprofloxacin with nano-biochar in saturated porous media: Impact of oxidized aging. Science of the Total Environment, 2021, 779, 146417.	8.0	18
52	Selective Leaching of Rare Earth Elements from Ion-Adsorption Rare Earth Tailings: A Synergy between CeO ₂ Reduction and Fe/Mn Stabilization. Environmental Science & Technology, 2021, 55, 11328-11337.	10.0	22
53	Kinetics, pathways and toxicity of hexabromocyclododecane biodegradation: Isolation of the novel bacterium Citrobacter sp. Y3. Chemosphere, 2021, 274, 129929.	8.2	10
54	Genome- and community-level interaction insights into the ecological role of archaea in rare earth element mine drainage in South China. Water Research, 2021, 201, 117331.	11.3	18

#	Article	IF	CITATIONS
55	Characterization of Neodymium Speciation in the Presence of Fulvic Acid by Ion Exchange Technique and Single Particle ICP-MS. Bulletin of Environmental Contamination and Toxicology, 2021, , 1.	2.7	1
56	Pathways to a more efficient and cleaner energy system in Guangdong-Hong Kong-Macao Greater Bay Area: A system-based simulation during 2015-2035. Resources, Conservation and Recycling, 2021, 174, 105835.	10.8	13
57	Simultaneous hyperaccumulation of rare earth elements, manganese and aluminum in Phytolacca americana in response to soil properties. Chemosphere, 2021, 282, 131096.	8.2	30
58	Experimental and DFT investigation on N-functionalized biochars for enhanced removal of Cr(VI). Environmental Pollution, 2021, 291, 118244.	7.5	15
59	Cable bacteria extend the impacts of elevated dissolved oxygen into anoxic sediments. ISME Journal, 2021, 15, 1551-1563.	9.8	41
60	Element Case Studies: Rare Earth Elements. Mineral Resource Reviews, 2021, , 471-483.	1.5	12
61	Plant-Soil Feedbacks for the Restoration of Degraded Mine Lands: A Review. Frontiers in Microbiology, 2021, 12, 751794.	3.5	17
62	Accelerated biodegradation of p-tert-butylphenol in the Phragmites australis rhizosphere by phenolic root exudates. Environmental and Experimental Botany, 2020, 169, 103891.	4.2	11
63	Effects of cadmium-resistant plant growth-promoting rhizobacteria and <i>Funneliformis mosseae</i> on the cadmium tolerance of tomato (<i>Lycopersicon esculentum</i> L.). International Journal of Phytoremediation, 2020, 22, 451-458.	3.1	27
64	Recovering full metallic resources from waste printed circuit boards: A refined review. Journal of Cleaner Production, 2020, 244, 118690.	9.3	117
65	Newly deposited atmospheric mercury in a simulated rice ecosystem in an active mercury mining region: High loading, accumulation, and availability. Chemosphere, 2020, 238, 124630.	8.2	21
66	Co-pyrolysis of sewage sludge and hydrochar with coals: Pyrolytic behaviors and kinetics analysis using TG-FTIR and a discrete distributed activation energy model. Energy Conversion and Management, 2020, 203, 112226.	9.2	43
67	Gallic acid accelerated BDE47 degradation in PMS/Fe(III) system: Oxidation intermediates autocatalyzed redox cycling of iron. Chemical Engineering Journal, 2020, 384, 123248.	12.7	64
68	Facile synthesis of Z-scheme composite of TiO2 nanorod/g-C3N4 nanosheet efficient for photocatalytic degradation of ciprofloxacin. Journal of Cleaner Production, 2020, 253, 120055.	9.3	180
69	Model-based rationalization of mixture toxicity and accumulation in Triticum aestivum upon concurrent exposure to yttrium, lanthanum, and cerium. Journal of Hazardous Materials, 2020, 389, 121940.	12.4	6
70	Inhibitory effects of metal ions on reductive dechlorination of polychlorinated biphenyls and perchloroethene in distinct organohalide-respiring bacteria. Environment International, 2020, 135, 105373.	10.0	31
71	High trans-placental transfer of perfluoroalkyl substances alternatives in the matched maternal-cord blood serum: Evidence from a birth cohort study. Science of the Total Environment, 2020, 705, 135885.	8.0	74
72	Debromination and Decomposition Mechanisms of Phenolic Resin Molecules in Ball Milling with Nano-Zerovalent Iron. ACS Sustainable Chemistry and Engineering, 2020, 8, 172-178.	6.7	22

#	Article	IF	CITATIONS
73	Ecological influences of the migration of micro resin particles from crushed waste printed circuit boards on the dumping soil. Journal of Hazardous Materials, 2020, 386, 121020.	12.4	14
74	Waste shrimp shell-derived hydrochar as an emergent material for methyl orange removal in aqueous solutions. Environment International, 2020, 134, 105340.	10.0	69
75	Coupling adsorption-photocatalytic reduction of Cr(VI) by metal-free N-doped carbon. Science of the Total Environment, 2020, 704, 135284.	8.0	49
76	Singlet oxygen mediated the selective removal of oxytetracycline in C/Fe3C/Fe0 system as compared to chloramphenicol. Environment International, 2020, 143, 105899.	10.0	34
77	Comparative Life-Cycle Assessment of Aquifer Thermal Energy Storage Integrated with in Situ Bioremediation of Chlorinated Volatile Organic Compounds. Environmental Science & Technology, 2020, 54, 3039-3049.	10.0	20
78	Reclamation with organic amendments and plants remodels the diversity and structure of bacterial community in ion-adsorption rare earth element mine tailings. Journal of Soils and Sediments, 2020, 20, 3669-3680.	3.0	14
79	Sludge pre-treatments change performance and microbiome in methanogenic sludge digesters by releasing different sludge organic matter. Bioresource Technology, 2020, 316, 123909.	9.6	11
80	Phytoextraction of rare earth elements from ion-adsorption mine tailings by Phytolacca americana: Effects of organic material and biochar amendment. Journal of Cleaner Production, 2020, 275, 122959.	9.3	32
81	Molecule co-fracture of organics in waste solar cells under different heating rates and the products analysis. Solar Energy Materials and Solar Cells, 2020, 214, 110573.	6.2	2
82	The influence on biosorption potentials of metal-resistant bacteria Enterobacter sp. EG16 and Bacillus subtilis DBM by typical red soil minerals. Journal of Soils and Sediments, 2020, 20, 3217-3229.	3.0	7
83	3D hierarchical H2-reduced Mn-doped CeO2 microflowers assembled from nanotubes as a high-performance Fenton-like photocatalyst for tetracycline antibiotics degradation. Applied Catalysis B: Environmental, 2020, 277, 119171.	20.2	260
84	Factors influencing heavy metal availability and risk assessment of soils at typical metal mines in Eastern China. Journal of Hazardous Materials, 2020, 400, 123289.	12.4	176
85	Phytostabilization of Cd and Pb in Highly Polluted Farmland Soils Using Ramie and Amendments. International Journal of Environmental Research and Public Health, 2020, 17, 1661.	2.6	34
86	Mobility of metal(loid)s in Pb/Zn tailings under different revegetation strategies. Journal of Environmental Management, 2020, 263, 110323.	7.8	17
87	A novel approach of accurately rationing adsorbent for capturing pollutants via chemistry calculation: Rationing the mass of CaCO3 to capture Br-containing substances in the pyrolysis of nonmetallic particles of waste printed circuit boards. Journal of Hazardous Materials, 2020, 393, 122410.	12.4	25
88	Robust Matrix Effect-Free Method for Simultaneous Determination of Legacy and Emerging Per- and Polyfluoroalkyl Substances in Crop and Soil Matrices. Journal of Agricultural and Food Chemistry, 2020, 68, 8026-8039.	5.2	11
89	Do toxicokinetic and toxicodynamic processes hold the same for light and heavy rare earth elements in terrestrial organism Enchytraeus crypticus?. Environmental Pollution, 2020, 262, 114234.	7.5	16
90	The shuttling effects and associated mechanisms of different types of iron oxide nanoparticles for Cu(II) reduction by Geobacter sulfurreducens. Journal of Hazardous Materials, 2020, 393, 122390.	12.4	13

#	Article	IF	CITATIONS
91	Enhanced removal of aqueous Cd(II) by a biochar derived from salt-sealing pyrolysis coupled with NaOH treatment. Applied Surface Science, 2020, 511, 145619.	6.1	42
92	Elucidating Toxicodynamic Differences at the Molecular Scale between ZnO Nanoparticles and ZnCl ₂ in <i>Enchytraeus crypticus</i> via Nontargeted Metabolomics. Environmental Science & Technology, 2020, 54, 3487-3498.	10.0	43
93	Recovery of the biological function of ethylenediaminetetraacetic acid-washed soils: Roles of environmental variations and microbes. Science of the Total Environment, 2020, 715, 137032.	8.0	16
94	Spatially Resolved Localization of Lanthanum and Cerium in the Rare Earth Element Hyperaccumulator Fern <i>Dicranopteris linearis</i> from China. Environmental Science & Technology, 2020, 54, 2287-2294.	10.0	31
95	Preparing cedrene from ethylene-vinyl acetate copolymer and polyethylene terephthalate of waste solar cells. Journal of Cleaner Production, 2020, 254, 120065.	9.3	8
96	Effects of Zn in sludge-derived biochar on Cd immobilization and biological uptake by lettuce. Science of the Total Environment, 2020, 714, 136721.	8.0	19
97	Mechanisms of Pb and/or Zn adsorption by different biochars: Biochar characteristics, stability, and binding energies. Science of the Total Environment, 2020, 717, 136894.	8.0	121
98	Interaction of Mn and Cd during their uptake in Celosia argentea differs between hydroponic and soil systems. Plant and Soil, 2020, 450, 323-336.	3.7	21
99	Accumulation and associated phytotoxicity of novel chlorinated polyfluorinated ether sulfonate in wheat seedlings. Chemosphere, 2020, 249, 126447.	8.2	38
100	Cadmium stable isotope variation in a mountain area impacted by acid mine drainage. Science of the Total Environment, 2019, 646, 696-703.	8.0	56
101	Ecological Risk Assessment of Neodymium and Yttrium on Rare Earth Element Mine Sites in Ganzhou, China. Bulletin of Environmental Contamination and Toxicology, 2019, 103, 565-570.	2.7	21
102	Phytotoxicity and oxidative effects of typical quaternary ammonium compounds on wheat (Triticum) Tj ETQq0 0	0 ggBT ∕Oʻ	verlgck 10 Tf
103	Synergistic effect of hydrothermal co-carbonization of sewage sludge with fruit and agricultural wastes on hydrochar fuel quality and combustion behavior. Waste Management, 2019, 100, 171-181.	7.4	107
104	Controls on rare-earth element transport in a river impacted by ion-adsorption rare-earth mining. Science of the Total Environment, 2019, 660, 697-704.	8.0	26
105	Phytoremediation of Lead and Chromium Contaminated Soil Improves with the Endogenous Phenolics and Proline Production in Parthenium, Cannabis, Euphorbia, and Rumex Species. Water, Air, and Soil Pollution, 2019, 230, 1.	2.4	56
106	Heat evolution and energy analysis of cyanide bioproduction by a cyanogenic microorganism with the potential for bioleaching of precious metals. Journal of Hazardous Materials, 2019, 377, 284-289.	12.4	35
107	Enhanced removal of Cr(VI) in the Fe(III)/natural polyphenols system: role of the in situ generated Fe(II). Journal of Hazardous Materials, 2019, 377, 321-329.	12.4	49
108	Directional concentration of bromine from nonmetallic particles of crushed waste printed circuit boards by vacuum-gasification-condensation. Journal of Cleaner Production, 2019, 231, 462-467.	9.3	24

#	Article	IF	CITATIONS
109	A cleaner and energy-saving technology of vacuum step-by-step reduction for recovering cobalt and nickel from spent lithium-ion batteries. Journal of Cleaner Production, 2019, 229, 1148-1157.	9.3	77
110	Could the rhizoplane biofilm of wetland plants lead to rhizospheric heavy metal precipitation and iron-sulfur cycle termination?. Journal of Soils and Sediments, 2019, 19, 3760-3772.	3.0	11
111	Potential impact of hydrodynamic shear force in aquifer thermal energy storage on dissolved organic matter releasement: A vigorous shaking batch study. Science of the Total Environment, 2019, 677, 263-271.	8.0	1
112	Vacuum pyrolysis method for reclamation of rare earth elements fromÂhyperaccumulator Dicranopteris dichotoma grown in contaminated soil. Journal of Cleaner Production, 2019, 229, 480-488.	9.3	30
113	Simultaneous attenuation of phytoaccumulation of Cd and As in soil treated with inorganic and organic amendments. Environmental Pollution, 2019, 250, 464-474.	7.5	36
114	Pyrolytic behavior and kinetic of wood sawdust at isothermal and non-isothermal conditions. Renewable Energy, 2019, 142, 284-294.	8.9	27
115	Effects of light irradiation on the complexes of cadmium and humic acids: The role of thiol groups. Chemosphere, 2019, 225, 174-181.	8.2	11
116	Two years of aging influences the distribution and lability of metal(loid)s in a contaminated soil amended with different biochars. Science of the Total Environment, 2019, 673, 245-253.	8.0	57
117	A resource-utilization way of the waste printed circuit boards to prepare silicon carbide nanoparticles and their photocatalytic application. Journal of Hazardous Materials, 2019, 373, 640-648.	12.4	26
118	Co-deposition of silicon with rare earth elements (REEs) and aluminium in the fern Dicranopteris linearis from China. Plant and Soil, 2019, 437, 427-437.	3.7	26
119	Controllable synthesis of mesoporous manganese oxide microsphere efficient for photo-Fenton-like removal of fluoroquinolone antibiotics. Applied Catalysis B: Environmental, 2019, 248, 298-308.	20.2	163
120	Single Ag atom engineered 3D-MnO2 porous hollow microspheres for rapid photothermocatalytic inactivation of E. coli under solar light. Applied Catalysis B: Environmental, 2019, 245, 177-189.	20.2	134
121	An ultrasensitive homogeneous aptasensor for carcinoembryonic antigen based on upconversion fluorescence resonance energy transfer. Talanta, 2019, 195, 33-39.	5.5	49
122	Heavy metals in human urine, foods and drinking water from an e-waste dismantling area: Identification of exposure sources and metal-induced health risk. Ecotoxicology and Environmental Safety, 2019, 169, 707-713.	6.0	82
123	Effects of the interactions between nickel and other trace metals on their accumulation in the hyperaccumulator Noccaea caerulescens. Environmental and Experimental Botany, 2019, 158, 73-79.	4.2	21
124	Different dynamic accumulation and toxicity of ZnO nanoparticles and ionic Zn in the soil sentinel organism Enchytraeus crypticus. Environmental Pollution, 2019, 245, 510-518.	7.5	24
125	Water, sediment and agricultural soil contamination from an ion-adsorption rare earth mining area. Chemosphere, 2019, 216, 75-83.	8.2	114
126	The effect of interaction between Bacillus subtilis DBM and soil minerals on Cu(II) and Pb(II) ads adsorption. Journal of Environmental Sciences, 2019, 78, 328-337.	6.1	25

#	Article	IF	CITATIONS
127	Insights into the surface chemistry of BioSeNPs produced by Bacillus lichenformis. , 2019, , 219-220.		0
128	Electron transport chains in organohalide-respiring bacteria and bioremediation implications. Biotechnology Advances, 2018, 36, 1194-1206.	11.7	108
129	A new model for simulating microbial cyanide production and optimizing the medium parameters for recovering precious metals from waste printed circuit boards. Journal of Hazardous Materials, 2018, 353, 135-141.	12.4	60
130	Wet torrefaction of biomass for high quality solid fuel production: A review. Renewable and Sustainable Energy Reviews, 2018, 91, 259-271.	16.4	163
131	Continuous leaching modifies the surface properties and metal(loid) sorption of sludge-derived biochar. Science of the Total Environment, 2018, 625, 731-737.	8.0	31
132	Characterization of the Materials in Waste Power Banks and the Green Recovery Process. ACS Sustainable Chemistry and Engineering, 2018, 6, 3815-3822.	6.7	36
133	Occurrence and fate of colloids and colloid-associated metals in a mining-impacted agricultural soil upon prolonged flooding. Journal of Hazardous Materials, 2018, 348, 56-66.	12.4	58
134	Phytoremediation of Heavy Metal-Contaminated Soil in Southern China. , 2018, , 375-387.		1
135	Nickel hyperaccumulation mechanisms: a review on the current state of knowledge. Plant and Soil, 2018, 423, 1-11.	3.7	67
136	Accumulation and fractionation of rare earth elements (REEs) in the naturally grown <i>Phytolacca americana</i> L. in southern China. International Journal of Phytoremediation, 2018, 20, 415-423.	3.1	59
137	Ecosystem services provided by heavy metal-contaminated soils in China. Journal of Soils and Sediments, 2018, 18, 380-390.	3.0	19
138	Effect of low-molecular-weight organic acids on hematite dissolution promoted by desferrioxamine B. Environmental Science and Pollution Research, 2018, 25, 163-173.	5.3	10
139	A novel pneumatic separator for separating diode and CD capacitance of waste printed circuit boards. Energy, 2018, 142, 191-195.	8.8	5
140	Element Case Studies: Rare Earth Elements. Mineral Resource Reviews, 2018, , 297-308.	1.5	26
141	Encapsulating nanoscale zero-valent iron with a soluble Mg(OH) ₂ shell for improved mobility and controlled reactivity release. Journal of Materials Chemistry A, 2018, 6, 2517-2526.	10.3	35
142	Variation of the Bacterial Community in the Rhizoplane Iron Plaque of the Wetland Plant Typha latifolia. International Journal of Environmental Research and Public Health, 2018, 15, 2610.	2.6	8
143	Hyperaccumulator Plants from China: A Synthesis of the Current State of Knowledge. Environmental Science & Technology, 2018, 52, 11980-11994.	10.0	180
144	Elements in the Crystals Determine the Distribution of Bromine in Nonmetallic Particles of Crushed Waste Printed Circuit Boards. ACS Sustainable Chemistry and Engineering, 2018, 6, 13650-13655.	6.7	18

#	Article	IF	CITATIONS
145	Scientific and Industrial Application of Plasma Fluidized Bed. Advanced Topics in Science and Technology in China, 2018, , 81-121.	0.1	3
146	Comparison of the Performance with Different Plasma Fluidized Beds. Advanced Topics in Science and Technology in China, 2018, , 123-138.	0.1	0
147	Recovery of rare earth elements from Dicranopteris dichotoma by an enhanced ion exchange leaching process. Chemical Engineering and Processing: Process Intensification, 2018, 130, 208-213.	3.6	71
148	Heat Transfer and Mass Transfer in the Plasma Fluidized Bed. Advanced Topics in Science and Technology in China, 2018, , 71-79.	0.1	0
149	Adsorption-reduction removal of Cr(VI) by tobacco petiole pyrolytic biochar: Batch experiment, kinetic and mechanism studies. Bioresource Technology, 2018, 268, 149-157.	9.6	152
150	Two-stage multi-fraction first-order kinetic modeling for soil Cd extraction by EDTA. Chemosphere, 2018, 211, 1035-1042.	8.2	11
151	Structural development and assembly patterns of the root-associated microbiomes during phytoremediation. Science of the Total Environment, 2018, 644, 1591-1601.	8.0	60
152	Contact Behavior between Cells and Particles in Bioleaching of Precious Metals from Waste Printed Circuit Boards. ACS Sustainable Chemistry and Engineering, 2018, 6, 11570-11577.	6.7	31
153	Potential of Cassia alata L. Coupled with Biochar for Heavy Metal Stabilization in Multi-Metal Mine Tailings. International Journal of Environmental Research and Public Health, 2018, 15, 494.	2.6	28
154	Thermal Plasma Fluidized Bed. Advanced Topics in Science and Technology in China, 2018, , 11-27.	0.1	0
155	Non-thermal Plasma Fluidized Bed. Advanced Topics in Science and Technology in China, 2018, , 29-35.	0.1	Ο
156	Discharge Characteristic in the Plasma Fluidized Bed. Advanced Topics in Science and Technology in China, 2018, , 51-55.	0.1	0
157	Hydrodynamics of Plasma Fluidized Bed. Advanced Topics in Science and Technology in China, 2018, , 57-69.	0.1	0
158	Influencing Factors on Understanding Plasma Fluidized Bed. Advanced Topics in Science and Technology in China, 2018, , 37-49.	0.1	0
159	Plasma Fluidized Bed. Advanced Topics in Science and Technology in China, 2018, , .	0.1	4
160	Applicative Ability and Environmental Risk. Advanced Topics in Science and Technology in China, 2018, , 139-143.	0.1	0
161	Surfactant-facilitated dechlorination of 2,2′,5,5′-tetrachlorinated biphenyl using zero-valent iron in soil/sediment solution: Integrated effects of plausible factors. Chemosphere, 2018, 212, 845-852.	8.2	12
162	Kinetics and mechanisms of the degradation of PPCPs by zero-valent iron (Fe°) activated peroxydisulfate (PDS) system in groundwater. Journal of Hazardous Materials, 2018, 357, 207-216.	12.4	79

#	Article	IF	CITATIONS
163	Stable isotope fractionation of zinc and cadmium in soil-plant system: A review. Chinese Science Bulletin, 2018, 63, 2944-2953.	0.7	0
164	Development of a buried bag technique to study biochars incorporated in a compost or composting medium. Journal of Soils and Sediments, 2017, 17, 656-664.	3.0	7
165	Effect of E-waste Recycling on Urinary Metabolites of Organophosphate Flame Retardants and Plasticizers and Their Association with Oxidative Stress. Environmental Science & Technology, 2017, 51, 2427-2437.	10.0	122
166	Immobilization of Cu by Bacillus subtilis DBM and the Role of Extracellular Polymeric Substances. Water, Air, and Soil Pollution, 2017, 228, 1.	2.4	8
167	Mechanisms of Fe biofortification and mitigation of Cd accumulation in rice (Oryza sativa L.) grown hydroponically with Fe chelate fertilization. Chemosphere, 2017, 175, 275-285.	8.2	42
168	Degradation of 2,2′,4,4′-tetrabromodiphenyl ether (BDE-47) by a nano zerovalent iron-activated persulfate process: The effect of metal ions. Chemical Engineering Journal, 2017, 317, 613-622.	12.7	57
169	Vacuum-Gasification-Condensation of Waste Toner To Produce Industrial Chemicals and Nanomaterials. ACS Sustainable Chemistry and Engineering, 2017, 5, 4923-4929.	6.7	36
170	Timeâ€dependent uptake and toxicity of nickel to <i>Enchytraeus crypticus</i> in the presence of humic acid and fulvic acid. Environmental Toxicology and Chemistry, 2017, 36, 3019-3027.	4.3	10
171	Effects of dissolved organic matter derived from forest leaf litter on biodegradation of phenanthrene in aqueous phase. Journal of Hazardous Materials, 2017, 324, 516-525.	12.4	38
172	Non-thermal plasma technology for organic contaminated soil remediation: A review. Chemical Engineering Journal, 2017, 313, 157-170.	12.7	140
173	The accumulation and fractionation of Rare Earth Elements in hydroponically grown Phytolacca americana L Plant and Soil, 2017, 421, 67-82.	3.7	49
174	Study of the Process and Mechanism of the Remediation of Phenol Contaminated Soil by Plasma Vibrated Bed. Plasma Chemistry and Plasma Processing, 2017, 37, 1635-1653.	2.4	4
175	Zerovalent iron in conjunction with surfactants to remediate sediments contaminated by polychlorinated biphenyls and nickel. Chemosphere, 2017, 189, 479-488.	8.2	12
176	Mitigation of Cd accumulation in paddy rice (Oryza sativa L.) by Fe fertilization. Environmental Pollution, 2017, 231, 549-559.	7.5	68
177	Growth and Cd uptake by rice (Oryza sativa) in acidic and Cd-contaminated paddy soils amended with steel slag. Chemosphere, 2017, 189, 247-254.	8.2	78
178	Metal Immobilization on Woodâ€Đerived Biochars: Distribution and Reactivity of Carbonate Phases. Journal of Environmental Quality, 2017, 46, 845-854.	2.0	16
179	Metal-tolerant Enterobacter sp. strain EG16 enhanced phytoremediation using Hibiscus cannabinus via siderophore-mediated plant growth promotion under metal contamination. Plant and Soil, 2017, 413, 203-216.	3.7	56
180	Environment-Friendly Technology of Recovering Full Resources of Waste Capacitors. ACS Sustainable Chemistry and Engineering, 2017, 5, 287-293.	6.7	16

#	Article	IF	CITATIONS
181	Effects of an iron-silicon material, a synthetic zeolite and an alkaline clay on vegetable uptake of As and Cd from a polluted agricultural soil and proposed remediation mechanisms. Environmental Geochemistry and Health, 2017, 39, 353-367.	3.4	44
182	Metal immobilization by sludge-derived biochar: roles of mineral oxides and carbonized organic compartment. Environmental Geochemistry and Health, 2017, 39, 379-389.	3.4	27
183	Carboxylesterase-involved metabolism of di-n-butyl phthalate in pumpkin (Cucurbita moschata) seedlings. Environmental Pollution, 2017, 220, 421-430.	7.5	39
184	OsARM1, an R2R3 MYB Transcription Factor, Is Involved in Regulation of the Response to Arsenic Stress in Rice. Frontiers in Plant Science, 2017, 8, 1868.	3.6	150
185	Effects of alkaline and bioorganic amendments on cadmium, lead, zinc, and nutrient accumulation in brown rice and grain yield in acidic paddy fields contaminated with a mixture of heavy metals. Environmental Science and Pollution Research, 2016, 23, 23551-23560.	5.3	19
186	Root Iron Plaque on Wetland Plants as a Dynamic Pool of Nutrients and Contaminants. Advances in Agronomy, 2016, 138, 1-96.	5.2	126
187	Structure, Variation, and Co-occurrence of Soil Microbial Communities in Abandoned Sites of a Rare Earth Elements Mine. Environmental Science & Technology, 2016, 50, 11481-11490.	10.0	163
188	Responses of Carbonic Anhydrase to Cadmium in the Zinc/Cadmium Hyperaccumulator Picris divaricata Vant Pedosphere, 2016, 26, 709-716.	4.0	13
189	Effect of coexisting Al(III) ions on Pb(II) sorption on biochars: Role of pH buffer and competition. Chemosphere, 2016, 161, 438-445.	8.2	28
190	Transcriptional up-regulation of genes involved in photosynthesis of the Zn/Cd hyperaccumulator Sedum alfredii in response to zinc and cadmium. Chemosphere, 2016, 164, 190-200.	8.2	49
191	Integration of organohalide-respiring bacteria and nanoscale zero-valent iron (Bio-nZVI-RD): A perfect marriage for the remediation of organohalide pollutants?. Biotechnology Advances, 2016, 34, 1384-1395.	11.7	67
192	Nickel translocation via the phloem in the hyperaccumulator Noccaea caerulescens (Brassicaceae). Plant and Soil, 2016, 404, 35-45.	3.7	52
193	Associations between polycyclic aromatic hydrocarbon (PAH) exposure and oxidative stress in people living near e-waste recycling facilities in China. Environment International, 2016, 94, 161-169.	10.0	116
194	Zinc Isotope Fractionation in the Hyperaccumulator <i>Noccaea caerulescens</i> and the Nonaccumulating Plant <i>Thlaspi arvense</i> at Low and High Zn Supply. Environmental Science & Technology, 2016, 50, 8020-8027.	10.0	36
195	Stabilization of cationic and anionic metal species in contaminated soils using sludge-derived biochar. Chemosphere, 2016, 149, 263-271.	8.2	116
196	Urinary Concentrations of Bisphenols and Their Association with Biomarkers of Oxidative Stress in People Living Near E-Waste Recycling Facilities in China. Environmental Science & Technology, 2016, 50, 4045-4053.	10.0	157
197	Survival Strategies of the Plant-Associated Bacterium Enterobacter sp. Strain EG16 under Cadmium Stress. Applied and Environmental Microbiology, 2016, 82, 1734-1744.	3.1	101
198	Investigating speciation and toxicity of heavy metals in anoxic marine sediments—a case study from a mariculture bay in Southern China. Journal of Soils and Sediments, 2016, 16, 665-676.	3.0	11

#	Article	IF	CITATIONS
199	Subcellular distribution and uptake mechanism of di-n-butyl phthalate in roots of pumpkin (Cucurbita) Tj ETQq1 1	9.784314 5.3	rgBT /Ove
200	Sludge-Derived Biochar for Arsenic(III) Immobilization: Effects of Solution Chemistry on Sorption Behavior. Journal of Environmental Quality, 2015, 44, 1119-1126.	2.0	67
201	Atrazine immobilization on sludge derived biochar and the interactive influence of coexisting Pb(II) or Cr(VI) ions. Chemosphere, 2015, 134, 438-445.	8.2	67
202	Synergistical enhancement by Ni2+ and Tween-80 of nanoscale zerovalent iron dechlorination of 2,2',5,5'-tetrachlorinated biphenyl in aqueous solution. Environmental Science and Pollution Research, 2015, 22, 555-564.	5.3	8
203	Pb(II), Cr(VI) and atrazine sorption behavior on sludge-derived biochar: role of humic acids. Environmental Science and Pollution Research, 2015, 22, 16031-16039.	5.3	44
204	Agromining: Farming for Metals in the Future?. Environmental Science & Technology, 2015, 49, 4773-4780.	10.0	243
205	The roles of humic substances in the interactions of phenanthrene and heavy metals on the bentonite surface. Journal of Soils and Sediments, 2015, 15, 1463-1472.	3.0	33
206	The photocatalytic interaction of Cr(VI) ions and phenol on polymer-modified TiO2 under visible light irradiation. Kinetics and Catalysis, 2015, 56, 569-573.	1.0	14
207	Gasification of corn cob using non-thermal arc plasma. International Journal of Hydrogen Energy, 2015, 40, 12634-12649.	7.1	48
208	Influences of organic compounds on the visible light induced photocatalytic reduction of Cr(VI). Kinetics and Catalysis, 2014, 55, 793-797.	1.0	5
209	Spatial heterogeneity effects of Zn/Cd-contaminated soil on the removal efficiency by the hyperaccumulator Sedum alfredii. Journal of Soils and Sediments, 2014, 14, 948-954.	3.0	8
210	Influence of the selective EDTA derivative phenyldiaminetetraacetic acid on the speciation and extraction of heavy metals from a contaminated soil. Chemosphere, 2014, 109, 1-6.	8.2	32
211	Migration and Stabilization of Multiple Heavy Metals in an Aged Contaminated Soil under a Constant Voltage Electric Field. Soil and Sediment Contamination, 2014, 23, 540-556.	1.9	6
212	Gold nanoparticles inducing surface disorders of titanium dioxide photoanode for efficient water splitting. Nano Energy, 2014, 10, 313-321.	16.0	42
213	Cadmium–zinc exchange and their binary relationship in the structure of Zn-related proteins: a mini review. Metallomics, 2014, 6, 1313-1323.	2.4	70
214	Biosorption mechanisms involved in immobilization of soil Pb by Bacillus subtilis DBM in a multi-metal-contaminated soil. Journal of Environmental Sciences, 2014, 26, 2056-2064.	6.1	105
215	Nickel and Zinc Isotope Fractionation in Hyperaccumulating and Nonaccumulating Plants. Environmental Science & Technology, 2014, 48, 11926-11933.	10.0	100
216	PAHs Sorption and Desorption on Soil Influenced by Pine Needle Litter-Derived Dissolved Organic Matter. Pedosphere, 2014, 24, 575-584.	4.0	30

#	Article	IF	CITATIONS
217	A Fuzzy-based Methodology for an Aggregative Environmental Risk Assessment of Restored Soil. Pedosphere, 2014, 24, 220-231.	4.0	8
218	NiO decorated Mo:BiVO4 photoanode with enhanced visible-light photoelectrochemical activity. International Journal of Hydrogen Energy, 2014, 39, 4820-4827.	7.1	72
219	Heavy metal immobilization by chemical amendments in polluted soils and influence on jute growth. WIT Transactions on Engineering Sciences, 2014, , .	0.0	0
220	Pb(II) and Cr(VI) sorption by biochars pyrolyzed from the municipal wastewater sludge under different heating conditions. Bioresource Technology, 2013, 147, 545-552.	9.6	175
221	Chelant extraction of heavy metals from contaminated soils using new selective EDTA derivatives. Journal of Hazardous Materials, 2013, 262, 464-471.	12.4	57
222	Degradation pathway of malachite green in a novel dual-tank photoelectrochemical catalytic reactor. Journal of Hazardous Materials, 2013, 260, 585-592.	12.4	48
223	Impaired leaf CO2 diffusion mediates Cd-induced inhibition of photosynthesis in the Zn/Cd hyperaccumulator Picris divaricata. Plant Physiology and Biochemistry, 2013, 73, 70-76.	5.8	30
224	Characterization of sewage sludge-derived biochars from different feedstocks and pyrolysis temperatures. Journal of Analytical and Applied Pyrolysis, 2013, 102, 137-143.	5.5	300
225	Silane-based coatings on the pyrite for remediation of acid mine drainage. Water Research, 2013, 47, 4391-4402.	11.3	76
226	Visible Light Induced Photocatalytic Degradation of Br-Trihalomethanes over Polymer-Modified TiO ₂ . Advanced Materials Research, 2013, 726-731, 2372-2375.	0.3	0
227	Cellular Tolerance, Accumulation and Distribution of Cadmium in Leaves of Hyperaccumulator Picris divaricata. Pedosphere, 2012, 22, 497-507.	4.0	22
228	Ruthenium dyes with heteroleptic tridentate 2,6-bis(benzimidazol-2-yl)-pyridine for dye-sensitized solar cells: Enhancement in performance through structural modifications. Inorganica Chimica Acta, 2012, 392, 388-395.	2.4	15
229	Fractionation of Stable Zinc Isotopes in the Field-Grown Zinc Hyperaccumulator Noccaea caerulescens and the Zinc-Tolerant Plant Silene vulgaris. Environmental Science & Technology, 2012, 46, 9972-9979.	10.0	45
230	Relative distribution of Pb2+ sorption mechanisms by sludge-derived biochar. Water Research, 2012, 46, 854-862.	11.3	886
231	Visible light induced photocatalytic reduction of Cr(VI) over polymer-sensitized TiO2 and its synergism with phenol oxidation. Water Research, 2012, 46, 2299-2306.	11.3	100
232	Enhanced adsorption and photocatalytic activity of BiOl–MWCNT composites towards organic pollutants in aqueous solution. Journal of Hazardous Materials, 2012, 229-230, 72-82.	12.4	90
233	Bioremediation of Contaminated Soil and Water. Pedosphere, 2012, 22, 425.	4.0	2
234	Designing Cropping Systems for Metal-Contaminated Sites: A Review. Pedosphere, 2012, 22, 470-488.	4.0	97

#	Article	IF	CITATIONS
235	Attenuation of Metal Bioavailability in Acidic Multi-Metal Contaminated Soil Treated with Fly Ash and Steel Slag. Pedosphere, 2012, 22, 544-553.	4.0	38
236	Mechanisms of Cd Hyperaccumulation and Detoxification in Heavy Metal Hyperaccumulators: How Plants Cope with Cd. Progress in Botany Fortschritte Der Botanik, 2012, , 127-159.	0.3	4
237	Electro-migration of heavy metals in an aged electroplating contaminated soil affected by the coexisting hexavalent chromium. Chemosphere, 2012, 86, 809-816.	8.2	28
238	Simultaneous extraction of Cr(VI) and Cu(II) from humic acid with new synthesized EDTA derivatives. Chemosphere, 2012, 88, 730-735.	8.2	12
239	The effects of radial oxygen loss on arsenic tolerance and uptake in rice and on its rhizosphere. Environmental Pollution, 2012, 165, 109-117.	7.5	95
240	Silicon-mediated amelioration of zinc toxicity in rice (Oryza sativa L.) seedlings. Plant and Soil, 2012, 350, 193-204.	3.7	98
241	Operational Conditions of Chelant-Enhanced Soil Washing for Remediation of Metal-Contaminated Soil. , 2012, , 59-91.		6
242	Organic acids in two arsenic hyperaccumulators and a non-hyperaccumulator of <i>Pteris</i> exposed to elevated arsenic concentrations. International Journal of Environmental Analytical Chemistry, 2011, 91, 241-254.	3.3	3
243	How Phytohormone Iaa and Chelator Edta Affect Lead Uptake by ZN/CD Hyperaccumulator <i>Picris Divaricata</i> . International Journal of Phytoremediation, 2011, 13, 1024-1036.	3.1	50
244	Phytostabilization Potential of <i>Jatropha Curcas</i> L. in Polymetallic Acid Mine Tailings. International Journal of Phytoremediation, 2011, 13, 788-804.	3.1	117
245	Evidence of high PM2.5 strong acidity in ammonia-rich atmosphere of Guangzhou, China: Transition in pathways of ambient ammonia to form aerosol ammonium at [NH4+]/[SO42–] = 1.5. Atmospheric Research, 2011, 99, 488-495.	4.1	81
246	Effects of Zn on plant tolerance and non-protein thiol accumulation in Zn hyperaccumulator Arabis paniculata Franch. Environmental and Experimental Botany, 2011, 70, 227-232.	4.2	28
247	Cadmium accumulation in and tolerance of rice (Oryza sativa L.) varieties with different rates of radial oxygen loss. Environmental Pollution, 2011, 159, 1730-1736.	7.5	104
248	Photocatalytic reduction of CO2 to hydrocarbons using AgBr/TiO2 nanocomposites under visible light. Catalysis Today, 2011, 175, 256-263.	4.4	158
249	The differentially-expressed proteome in Zn/Cd hyperaccumulator Arabis paniculata Franch. in response to Zn and Cd. Chemosphere, 2011, 82, 321-328.	8.2	47
250	Mitigation effects of silicon rich amendments on heavy metal accumulation in rice (Oryza sativa L.) planted on multi-metal contaminated acidic soil. Chemosphere, 2011, 83, 1234-1240.	8.2	256
251	Effects of humus on the environmental activity of mineral-bound Hg: influence on Hg plant uptake. Journal of Soils and Sediments, 2011, 11, 959-967.	3.0	7
252	Interaction of cadmium and zinc on accumulation and sub-cellular distribution in leaves of hyperaccumulator Potentilla griffithii. Journal of Hazardous Materials, 2011, 186, 1425-1430.	12.4	65

#	Article	IF	CITATIONS
253	Metal Mobility and Fraction Distribution in a Multimetal Contaminated Soil Chemically Stabilized with Different Agents. Journal of Hazardous, Toxic, and Radioactive Waste, 2011, 15, 266-274.	2.0	11
254	Removal of trace and major metals by soil washing with Na2EDTA and oxalate. Journal of Soils and Sediments, 2010, 10, 45-53.	3.0	70
255	Root foraging for zinc and cadmium requirement in the Zn/Cd hyperaccumulator plant Sedum alfredii. Plant and Soil, 2010, 327, 365-375.	3.7	60
256	Heavy metal (Pb, Zn) uptake and chemical changes in rhizosphere soils of four wetland plants with different radial oxygen loss. Journal of Environmental Sciences, 2010, 22, 696-702.	6.1	41
257	Effects of pyrene and fluoranthene on the degradation characteristics of phenanthrene in the cometabolism process by Sphingomonas sp. strain PheB4 isolated from mangrove sediments. Marine Pollution Bulletin, 2010, 60, 2043-2049.	5.0	24
258	Constitutional tolerance to heavy metals of a fiber crop, ramie (Boehmeria nivea), and its potential usage. Environmental Pollution, 2010, 158, 551-558.	7.5	68
259	Effect of arsenic on flavonoid contents in Pteris species. Biochemical Systematics and Ecology, 2010, 38, 529-537.	1.3	19
260	Influence of EDTA washing on the species and mobility of heavy metals residual in soils. Journal of Hazardous Materials, 2010, 173, 369-376.	12.4	181
261	Influence of soil washing with a chelator on subsequent chemical immobilization of heavy metals in a contaminated soil. Journal of Hazardous Materials, 2010, 178, 578-587.	12.4	69
262	Cadmium tolerance of carbon assimilation enzymes and chloroplast in Zn/Cd hyperaccumulator Picris divaricata. Journal of Plant Physiology, 2010, 167, 81-87.	3.5	132
263	Characterization of the Sesbania rostrata Phytochelatin Synthase Gene: Alternative Splicing and Function of Four Isoforms. International Journal of Molecular Sciences, 2009, 10, 3269-3282.	4.1	13
264	Lead, zinc, cadmium hyperaccumulation and growth stimulation in Arabis paniculata Franch. Environmental and Experimental Botany, 2009, 66, 126-134.	4.2	184
265	Tolerance, accumulation and distribution of zinc and cadmium in hyperaccumulator Potentilla griffithii. Environmental and Experimental Botany, 2009, 66, 317-325.	4.2	111
266	Responses of non-protein thiols to Cd exposure in Cd hyperaccumulator Arabis paniculata Franch. Environmental and Experimental Botany, 2009, 66, 242-248.	4.2	61
267	Acid deposition critical loads modeling for the simulation of sulfur exceedance and reduction in Guangdong, China. Journal of Environmental Sciences, 2009, 21, 1108-1117.	6.1	2
268	Performance and kinetic evaluation of anaerobic moving bed biofilm reactor for treating milk permeate from dairy industry. Bioresource Technology, 2009, 100, 5641-5647.	9.6	75
269	Role of oxygen active species in the photocatalytic degradation of phenol using polymer sensitized TiO2 under visible light irradiation. Journal of Hazardous Materials, 2009, 163, 843-847.	12.4	121
270	Sulfate reduction and copper precipitation by a Citrobacter sp. isolated from a mining area. Journal of Hazardous Materials, 2009, 164, 1310-1315.	12.4	56

#	Article	IF	CITATIONS
271	The study of operating variables in soil washing with EDTA. Environmental Pollution, 2009, 157, 229-236.	7.5	194
272	Treatability and kinetic analysis of anaerobic moving bed biofilm reactor treating high strength milk permeate. Desalination and Water Treatment, 2009, 4, 191-197.	1.0	7
273	Zn and Cd hyperaccumulating characteristics of Picris divaricata Vant International Journal of Environment and Pollution, 2009, 38, 26.	0.2	32
274	Effects of exogenous citric acid and malic acid addition on nickel uptake and translocation in leaf mustard (Brassica juncea var. foliosa Bailey) and Alyssum corsicum. International Journal of Environment and Pollution, 2009, 38, 15.	0.2	7
275	Visible light induced photocatalytic degradation of phenol by polymer-modified semiconductors: Study of the influencing factors and the kinetics. Reaction Kinetics and Catalysis Letters, 2008, 94, 183-189.	0.6	10
276	Photocatalytic activity of polymer-modified ZnO under visible light irradiation. Journal of Hazardous Materials, 2008, 156, 80-85.	12.4	208
277	Antioxidative response to Cd in a newly discovered cadmium hyperaccumulator, Arabis paniculata F Chemosphere, 2008, 74, 6-12.	8.2	123
278	Characterization of Conjugated Polymer Poly(fluorene-co-thiophene) and Its Application as Photosensitizer of <mml:math <br="" xmlns:mml="http://www.w3.org/1998/Math/MathML">id="E1"><mml:mrow><mml:msub><mml:mrow><mml:mtext>TiO</mml:mtext></mml:mrow><mml:mtext>2International Journal of Photoenergy, 2008, 2008, 1-5.</mml:mtext></mml:msub></mml:mrow></mml:math>	ml:mtext>	
279	Effective removal of coordinated copper from wastewater using a new dithiocarbamate-type supramolecular heavy metal precipitant. Chemosphere, 2007, 69, 1783-1789.	8.2	87
280	Photodegradation of phenol in a polymer-modified TiO2 semiconductor particulate system under the irradiation of visible light. Catalysis Communications, 2007, 8, 429-433.	3.3	116
281	Water eutrophication in China and the combating strategies. Journal of Chemical Technology and Biotechnology, 2007, 82, 781-786.	3.2	109
282	Response of microbial communities to phytoremediation of nickel contaminated soils. Frontiers of Agriculture in China, 2007, 1, 289-295.	0.2	5
283	Removal of NOx by microwave reactor with ammonium bicarbonate and Ga-A zeolites at low temperature. Energy, 2007, 32, 1455-1459.	8.8	21
284	Zinc Hyperaccumulation and Uptake by <i>Potentilla Griffithii</i> Hook. International Journal of Phytoremediation, 2006, 8, 299-310.	3.1	38
285	Simultaneous photocatalytic reduction of Cr(VI) and oxidation of phenol over monoclinic BiVO4 under visible light irradiation. Chemosphere, 2006, 63, 956-963.	8.2	175
286	Development of microsatellite markers in a mangrove tree species Aegiceras corniculatum (Myrsinaceae). Molecular Ecology Notes, 2006, 6, 1231-1233.	1.7	5
287	Lead, zinc and cadmium accumulation in herbaceous species and soils in Lanping Pb/Zn mining area, Yunnan Province, China. Diqiu Huaxue, 2006, 25, 250-250.	0.5	4
288	Contents and Leaching of Trihalomethane Precursors in Soils. Water, Air, and Soil Pollution, 2003, 145, 35-52.	2.4	3

#	Article	IF	CITATIONS
289	Visible Light Induced Photocatalytic Degradation of Rhodamine B in the Presence of Cr(VI). Applied Mechanics and Materials, 0, 295-298, 1434-1437.	0.2	Ο
290	Colloidal stabilities and deposition behaviors of chromium (hydr)oxides in the presence of dissolved organic matters: role of coprecipitation and adsorption. Environmental Science: Nano, 0, , .	4.3	2